Research on Design and Ideal Variable Transmission Ratio Control of Distributed Steering-By-Wire System

Ruixue Wang, Kun Yang, Jun Guo, Chao Ma, Enbiao Chu and Yucheng Zhu

Abstract—**The Steer-by-wire (SBW) system is a key technology for chassis-by-wire, electric vehicles, and autonomous driving. However, conventional SBW remains mechanical connections between the left wheel and right wheel, which cannot achieve independent steering of two steering wheels. Therefore, DSBW has become a research hotspot for further improving vehicle steering performance and handling stability. For that, a DSBW scheme integrated fault-tolerant mechanism is proposed. Aiming at the failure problem of SBW, the fault-tolerant mechanism is designed. The demand for DSBW is analyzed. The parameter matching and selection of main components is carried out. 3D model is built, motion check is carried out based on CATIA and Adams/View, and the strength is checked under three extreme conditions. Taking the steering knuckle as example, the topology optimization is studied under the premise of ensuring the strength requirements and meeting demands of lightweighting. Considering the steering performance and handling stability of vehicle, the design of ideal variable transmission ratio for DSBW is studied to take advantages of adjustable steering transmission ratio of DSBW, and the corresponding comprehensive evaluation index is proposed. The optimal yaw rate gain is selected based on genetic algorithm, and the modified sine function is utilized to fit the ideal variable transmission ratio curve. For improving the adaptability of steering transmission ratio to road adhesion coefficients, the ideal variable transmission ratio on different road adhesion coefficients is modified based on fuzzy control. The results show that the weight of the steering knuckle is reduced by 6.7% after topology optimization, and the ideal variable transmission ratio can meet the requirements of steering portability at low speed and handling stability at high speed under continuous sine condition, step input condition, fishhook maneuver test and steady circular test.**

Index Terms—**steer-by-wire system, strength analysis, topology optimization, variable transmission ratio.**

Manuscript received February 8, 2025; revised July 9, 2025.

This work was supported by the Nature Science Foundation of Shandong Province (Grant No.ZR2024ME194), National Nature Science Foundation of China (Grant No.51605265), and Shandong Province Key Research and Development Program (Grant No.2018GGX105010).

Ruixue Wang is a postgraduate student of Shandong University of Technology, Zibo 255000 China (e-mail: a17686973140@163.com).

Kun Yang is a professor of Shandong University of Technology, Zibo 255000, China (Corresponding author to provide email: yangkun@sdut.edu.cn).

Jun Guo is an engineer of China National Heavy Duty Truck Group CO., LTD., Jining 272000, China (e-mail: guojun_sdut@163.com).

Chao Ma is a professor of Shandong University of Technology, Zibo 255000, China (e-mail: mc@sdut.edu.cn).

Enbiao Chu is a postgraduate student of Shandong University of Technology, Zibo 255000, China (e-mail: enbiao_sdut@163.com).

Yucheng Zhu is a postgraduate student of Shandong University of Technology, Zibo 255000, China (e-mail: 19546305236@163.com).

I. Introduction

Steer-by-Wire (SBW) is an advanced automotive steering technology. It cancels the conventional mechanical connection and transmits driver's steering intentions by electronic signals [1]. It has become the development direction of steering system for the following three reasons. First, the connections of the conventional steering column and related mechanical components are cancelled, and the greater riding space can be obtained [2]. Second, the advanced driver assistance system (ADAS) can be integrated to enhance the vehicle performance [3]. Third, the steering response can be improved significantly compared with conventional power steering [4]. Meanwhile, it also brings three problems. First, the connections between the conventional steering column and related mechanical components are cancelled, and the malfunction of the electronic system or steering motor will result in steering failure. Therefore, redundant systems are needed to ensure security, and this will increase the complexity and cost of SBW. Second, the steering mechanism withstands the load impact from all directions during the vehicle driving. For that, the material structure in the stress concentration area will change gradually, and this will result in fatigue cracks. Third, the mechanical connection between steering wheel and steering gear is eliminated, requiring the design of a reasonable transmission ratio to improve handling stability.

For the first problem, Shi et al. [5] proposed a kind of SBW with redundant motor. A dual-motor control architecture was proposed and the dual-motor global control was developed. A fault-diagnosis method and a fault-tolerant control strategy were designed. The simulation results show that the dual-motor actuator can better realize the synchronous operation. The dual-motor system can realize fast fault-isolation and smooth switching. Wang et al. [6] proposed a dual-motor structure for improving the fault-tolerant ability of SBW. Aiming at problem of high steering energy consumption caused by redundant motors, a dual-motor coupling steering (DMCS) strategy was proposed, and the steering energy could be minimized. The simulation results show that the DMCS strategy can satisfy the stability demands and realize the optimal energy allocation between two motors at different steering conditions, thereby improving energy utilization efficiency. However, the connection between two steering wheels is preserved, and the they cannot turn independently. This results in that the vehicle performance related to steering system cannot be improved effectively, so the distributed steer-by-wire (DSBW) system becomes another research hotspot. For the

second problem, Xu et al. [7] proposed the angle-based block partitioning symmetric model for design of steering linkage topology. The synergistic optimization for efficiency and accuracy was achieved. Compared with the conventional spring-connected block approach, the angular output mechanism design demonstrated superior convergence and accuracy. The simulation show that the rapid convergence of scheme is better in the steering linkage topology design. Shen et al. [8] conducted the multi-body dynamics analysis for the hydraulic power steering system of double front axles, and the load spectrums for the steering power cylinder bracket (SPCB) were analyzed under typical working conditions. Then, the nonlinear strength calculation and topology optimization analysis for the bracket were performed to select the optimal scheme. The simulation results show that the SPCB weight was reduced by about 2.53 kg, and the lightweight effect is significant. The steering knuckle is a key component that ensures precise response and reliability of steering system. During the steering process, it needs to withstand road impact loads in various directions, which makes its stress very complex and some of the impact loads are large. Therefore, its strength needs to be strengthened, but this will decrease the response speed during steering. The above problem can be solved by the topology optimization under the constraints of steering response speed and steering reliability, but the research for that is few currently.

For the third problem, Lin et al. [9] developed variable transmission ratio controller for conventional SBW. The vehicle velocity and steering wheel angle were utilized to adjust the variable transmission ratio. For harmonizing the transmission ratio weights, the coefficient of variation method was adopted, and a fuzzy neural network was adopted to design a nonlinear controller to control transmission ratio. The results show that the variable transmission ratio control of SBW alleviate the operational burden significantly, and the handling stability can be improved compared with traditional constant transmission ratio control. For improving the vehicle handling performance, Wu et al. [10] proposed a variable transmission ratio control for SBW. The transmission ratio of SBW was regulated by compensation coefficient. For evaluating the performance of variable transmission ratio, analyses were conducted based on quadratic cost functions of vehicle lateral offset, vehicle lateral acceleration, steering angular speed and roll angle. A Takagi-Sugeno fuzzy neural network was developed for the variable transmission ratio control based on the optimized data from the simulation results. The simulation results show that the proposed system can optimize low-speed sensitivity and high-speed stability, and it can alleviate driver's workload compared with the traditional steering system with constant transmission ratio. At present, the variable transmission ratio control of SBW refers to the influence of speed on handling stability. However, the road adhesion coefficient, steering wheel angle, vehicle velocity, and yaw rate gain value have significant impact on vehicle performance, so they should be mentioned in the variable transmission ratio control, but the related research is few.

For taking advantages of the SBW and addressing the aforementioned issues, a new DSBW scheme with two motors is designed. It consists of two steering motors, wedge block, ball screw, push rod and roller, etc. The fault tolerant mechanism is designed to solve its failure problem. Based on the requirements of DSBW, the parameter matching and selection of main components is carried out. 3D model is built, and motion check is carried out based on CATIA and Adams/View. Aiming at the complex force analysis, the strength check is carried out under typical limit conditions based on ANSYS Workbench. For improving the steering response speed and reducing material costs, topology optimization is carried out for the steering knuckle with goal of lightweighting. During the optimization process, the strength of the steering knuckle should meet the requirements. For improving vehicle steering performance and handling stability, an ideal variable transmission ratio calculation method based on the optimal vehicle velocity, yaw rate gain value, steering wheel angle, and road adhesion coefficient is proposed. The optimal yaw rate gain value is obtained through genetic algorithm. In order to reduce the deviation between the variable transmission ratio curve and the ideal variable transmission ratio curve, an improved S-function is applied to correct the ideal variable transmission ratio curve. For improving the adaptability of the steering transmission ratio to road adhesion coefficients, the ideal variable transmission ratio is obtained by fuzzy control. The performance of DSBW based on ideal variable transmission ratio is verified through continuous sine condition, step input condition and fishhook maneuver test.

II. DSBW Design

A. DSBW scheme

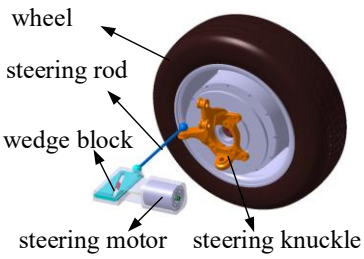

(a) Layout of DSBW

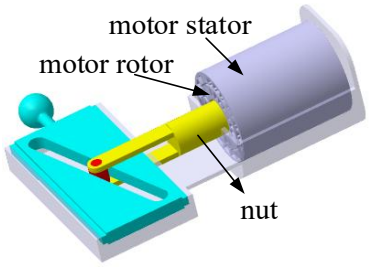

(b) Transmission mechanism

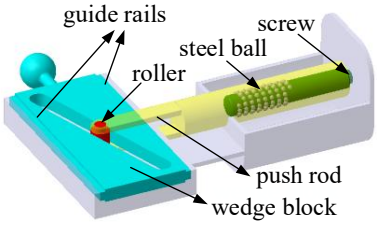

(c) Internal structure of transmission mechanism

Fig. 1. DSBW structural schematic diagram

For achieving independent steering of each steering wheel, a DSBW scheme is proposed, as Fig. 1 (a). The connection

between the left wheel and right wheel is eliminated and two steering wheels are driven by two independent steering motors. The DSBW consists of the steering knuckle, steering rod, and transmission device mainly. Its transmission mechanism mainly consists of the motor, ball screw, roller, push rod and wedge block. The motor consists of the motor rotor and motor stator. The ball screw is composed of nut, screw and steel ball, as Fig. 1(b) and (c). The screw is connected with motor rotor fixedly. For reducing the size of the transmission mechanism, the motor rotor is designed as hollow structure. The screw is used to transform the rotational motion of motor into linear motion, thereby pushing the nut to move along the screw's axial direction. The end of the nut is fixed with two parallel push rods. The roller is installed at the other end of the push rods and it can rotate around its axis freely. There is a through slot in the wedge block, and the roller rolls around its axis in the through slot, and its axis moves horizontally along its groove wall. There are guide rails on both sides of the wedge block, and the wedge block can only move along the axial direction of the guide rails. The ball pin of the wedge block is connected with steering rod, and the steering rod is connected with steering knuckle through the ball pin. The wheel rotates around the kingpin to steer under the pull of the steering rod. By setting the angle between the through slot and the wedge block guide rail reasonably, the working stroke of nut and the longitudinal dimension of the transmission mechanism can be reduced effectively.

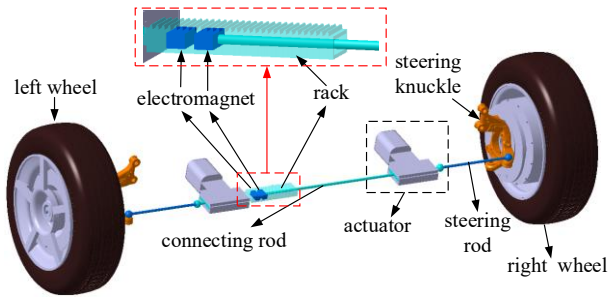

Fig. 2. Fault-tolerant mechanism of DSBW

For avoiding steering failure caused by steering motor failure, the fault-tolerant mechanism for DSBW is designed, as shown in Fig. 2. It consists of the electromagnet, rack, and connecting rod mainly. The electromagnet is disconnected, and the two wheels can steer independently when the DSBW on both sides can operate normally. When one or both steering motors fail, the push rod is disconnected from the nut. Two steering wheels are connected together by the electromagnet and connecting rod, and both steering wheels cannot steer independently at this time. The rack meshes with the conventional rack and pinion steering system through gears. When the driver rotates the steering wheel, the gear meshed with the rack rotates, and the rack moves along the connecting rod axis to achieve steering.

B. Parameter matching of DSBW

The maximum steering resistance torque in-situ is input for the parameter matching of DSBW actuators, which mainly includes the resistance of steering wheel rotating around kingpin and the resistance of tire deformation [11]. It is can calculated by semi-empirical formula, as equation 1.

$$M = \frac{f}{3}\sqrt{\frac{G^3}{p}} \tag{1}$$

where, M is the maximum steering resistance torque, f is the coefficient of friction between the tire and the ground, p is the tyre pressure, G is the load on steering axle.

The force on each component of the actuator is complex, because the structure is irregular [12]. For that, maximum required thrust is calculated based on the maximum steering resistance torque in-situ and the Adams/view model. The corresponding DSBW model for right front wheel and the constraints are shown in Fig. 3.

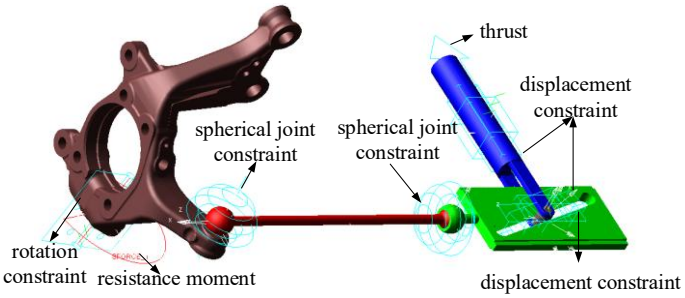

Fig. 3. DSBW model and the constraints

The parameter matching for ball screw and motor are taken as example for explanation. The rotation angle is positive when the wheel rotates counterclockwise. When the wheel resistance moment is 160N·m, the relationship between wheel angle and thrust of ball screw can be obtained based on the above model, as Fig. 4.

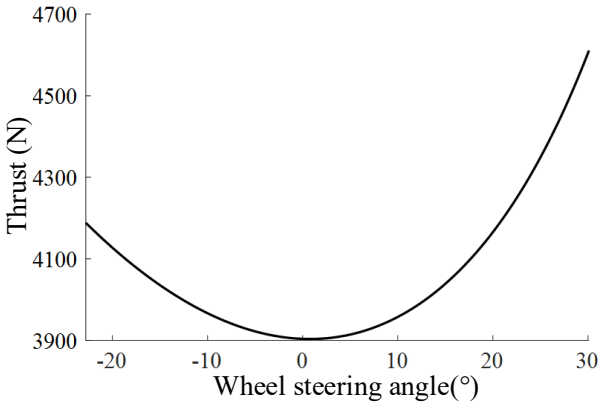

Fig. 4. Relationship of ball screw thrust and wheel angle

The HRBN FFZD1604-3 is adopted based on the maximum thrust requirement for the ball screw, and the key parameter values are shown in Table I.

TABLE I
BALL SCREW PARAMETERS

Parameters	Nominal diameter	Lead	Number of turns	Dynamic load	Static load
Value	16 mm	4 mm	3	4800 N	9700 N

The motor speed need to meet the requirements of the wheel steering speed [13]. The wheel steering speed is the maximum under the step input condition. Based on GB/T 6324-2014, the steering wheel angular speed is between 200 °/s and 360 °/s at this time, and the DSBW motor speed can be calculated accordingly. In addition, the variable

transmission ratio is one of characteristics of DSBW. From the perspective of balancing low-speed portability and high-speed stability effectively, the corresponding transmission ratio is set to 8-25. The relationship between wheel angular speed and steering wheel angle speed is as follows.

$$\omega_p = \frac{\omega_w}{i} \tag{2}$$

where, w_p is the wheel angular speed, w_w is the steering wheel angle speed, i is the transmission ratio of steering system.

Based on the developed DSBW model, the relationship between wheel angle and movement speed of ball screw nut can be obtained when the rotational speed of steering knuckle is given. For example, when the rotational speed of steering knuckle is 45 °/s, the relationship between the wheel angle and the movement speed of ball screw nut is shown in Fig. 5. Under these conditions, the maximum movement speed of ball screw nut is 32.19 mm/s.

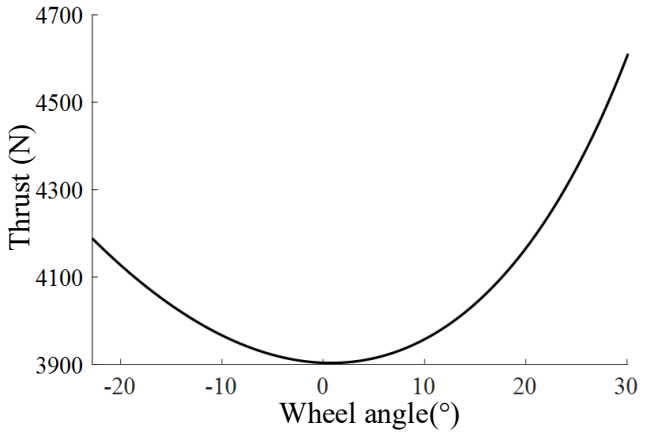

Fig. 5. Relationship of nut movement speed and wheel angle

The relationship between movement speed of ball screw nut and motor speed is shown as follows:

$$v_l = \frac{v_m l}{60} \tag{3}$$

where, v_l is the movement speed of ball screw nut, v_m is the motor speed, l is the lead of the ball screw.

Based on the above conditions, the main parameters of steering motor are shown in Table II.

TABLE II
PARAMETERS OF STEERING MOTOR

Parameters	Rated voltage	Rated power	Rated torque	Rated speed
Value	24 V	0.4 kW	4 Nm	1000 r/min

III. FINITE ELEMENT ANALYSIS

Aiming at the complex force analysis, the strength verification for DSBW is carried out under typical limit conditions based on ANSYS Workbench. Because the stress of steering knuckle is very complex, it is taken as an example for explanation.

A. Static analysis

During the driving, load borne by the steering knuckle is complex and large, which requires its strength to be high. For that, the typical extreme conditions such as uneven road condition, emergency braking condition, and sideslip condition are utilized for strength check of the steering knuckle.

1) *Uneven road condition:* When the vehicle is driving on uneven roads, the knuckle mainly withstands the vertical load from the ground, and the vertical load is large. Therefore, it is usually used to verify the vertical strength. Under these conditions, the vertical load borne by the steering knuckle is as follows.

$$F_z = \frac{1}{2} K_d G_f \tag{4}$$

where, F_z is the vertical load, K_d is the dynamic load factor, the G_f is the front axle load.

2) *Emergency braking condition:* During emergency braking on high adhesion road, the wheels withstand vertical and longitudinal force from the ground, both of which are significant and transmitted to steer knuckle. In addition, the steering knuckle also withstands additional moment along the longitudinal direction caused by the translation of the longitudinal load. The load borne by the steering knuckle is shown as follows.

$$F_x = F_z \varphi \tag{5}$$

$$F_z = \frac{1}{2} K_d G_f \tag{6}$$

$$M_y = F_x r \tag{7}$$

where, F_x is the longitudinal load borne by the steering knuckle, M_y is the additional moment, φ is the road coefficient adhesion, r is the rolling radius of tire, the other symbols are the same as above.

3) *Sideslip condition:* When the vehicle sideslips on the high adhesion road, the wheels withstand vertical and lateral forces from ground, both of which are significant and transmitted to the steering knuckle. In addition, the translation of lateral loads will also cause the additional moment for steering knuckle along the lateral direction. Under this extreme condition, the value of lateral force for left and right front wheels are different, and they are as follows.

$$F_{Ly} = \frac{1}{2} G_f \psi \left(\frac{2h_g \psi}{B} + 1\right) \tag{8}$$

$$F_{Ry} = \frac{1}{2} G_f \psi \left(\frac{2h_g \psi}{B} - 1\right) \tag{9}$$

where, F_{Ly} is the lateral force on left front wheel, F_{Ry} is the lateral force on right front wheel, ψ is the lateral slip adhesion coefficient, h_g is the height of center of mass, B is the front wheel tread, the other symbols are the same as above.

The left sideslip is taken as an example, the lateral force of left wheel is much greater than the right wheel. For that, the left steering knuckle is selected as the object for analysis, and the corresponding load borne by the left steering knuckle is as follows.

$$F_y = \frac{1}{2} G_f \psi \left(\frac{2h_g \psi}{B} + 1\right) \tag{10}$$

$$F_z = \frac{1}{2} G_f \left(\frac{2h_g \psi}{B} + 1\right) \quad (11)$$

$$M_x = F_y r \quad (12)$$

where, F_y is the lateral load on the steering knuckle, M_x is the additional moment, the other symbols are the same as above.

B. Results of strength check

The stress cloud diagram for the steering knuckle under each operating condition can be obtained based on CATIA and ANSYS Workbench. The corresponding work includes importing the 3D model of the steering knuckle into ANSYS Workbench, setting the constraints on the steering knuckle, and applying the corresponding load according to the working condition requirements.

1) *Uneven road condition:* The stress cloud diagram for uneven road condition as Fig. 6. The maximum stress occurs at the connection between the lower support table of the steering knuckle and the lower cross arm of the suspension. The maximum stress value is 38.634 MPa, and strength of designed steering knuckle meets the requirement.

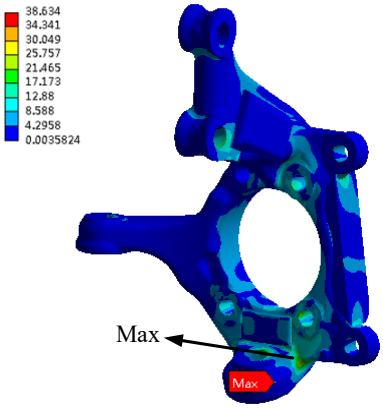

Fig. 6. Stress cloud diagram of uneven road condition

2) *Emergency braking condition:* The stress cloud diagram for emergency braking condition as Fig. 7. The maximum stress occurs at two lugs connected to the brake caliper. The maximum stress value is 93.484 MPa, and strength of designed steering knuckle meets the requirement.

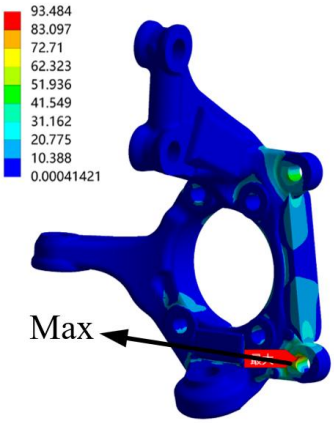

Fig. 7. Stress cloud diagram of emergency braking condition

3) *Sideslip condition:* The stress cloud diagram of the sideslip condition as Fig. 8. The maximum stress appeared at the connection between the lower support table of steering knuckle and the lower cross arm of suspension. The maximum stress value is 184.32 MPa, and strength of designed steering knuckle meets the requirement.

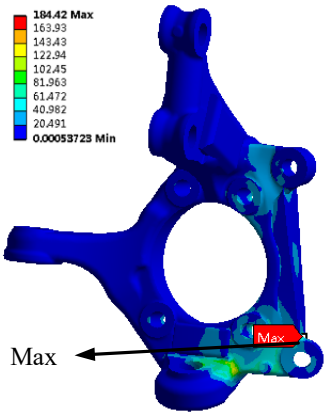

Fig. 8. Stress cloud diagram of sideslip condition

C. Topology optimization of the steering knuckle

For improving the steering response speed and reducing the material costs, the topology optimization of steering knuckle is carried out with the goal of lightweighting. During the optimization process, the strength of the steering knuckle should meet the requirements. The result as Fig. 9. The gray part is reserved part, and the red part is removable part.

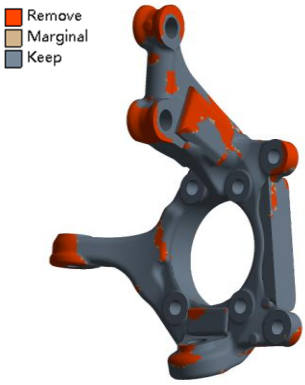

Fig. 9. Result of topology optimization

The steering knuckle structure is redesigned based on topology optimization results. The strength analysis for optimized steering knuckle is conducted under uneven road condition, emergency braking condition, and sideslip condition. The results as Fig. 10.

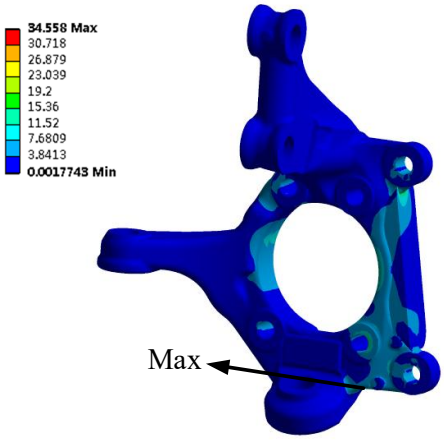

(a) Uneven road condition

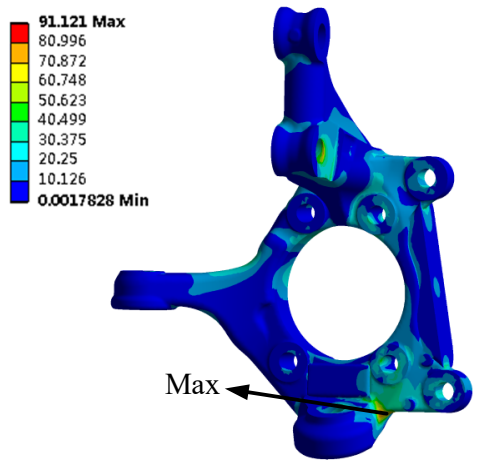

(b) Emergency braking condition

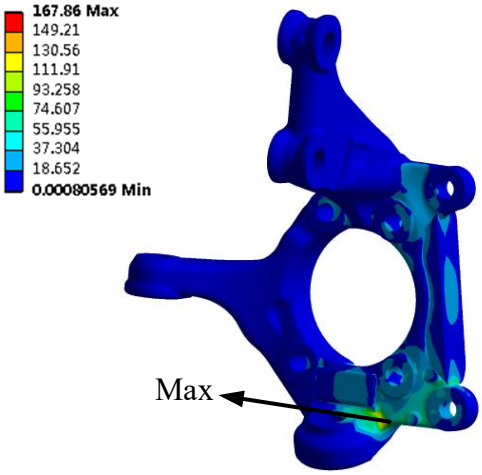

(c) Sideslip condition

Fig. 10. Stress cloud diagram of three conditions

As Fig. 10(a), the maximum stress value of steering knuckle after topology optimization is 34.5 MPa under uneven road condition, and it is reduced by 10.6%. As Fig. 10(b), the maximum stress value of the steering knuckle after topology optimization is 91.1 MPa under emergency braking condition, and it is reduced by 2.5%. As Fig. 10(c), the maximum stress value of the steering knuckle after topology optimization is 167.8 MPa under sideslip condition, and it is reduced by 9.0%. In addition, the weight of steering knuckle is reduced by 0.38 kg after topology optimization, and it is reduced by 6.7%.

IV. Ideal Variable Transmission Ratio Design for DSBW

A. Design of the ideal variable transmission ratio based on yaw rate gain

The transmission ratio for steering system can be calculated by follow equation.

$$i = \frac{\delta_{sw}}{\delta_f} \tag{13}$$

where, δ_{sw} is the steering wheel angle, δ_f is the front wheel angle, the other symbols are the same as above.

The steering characteristics of vehicle is characterized by yaw rate gain [14]. The yaw rate gain can be calculated by following equation.

$$G_{sw} = \frac{\omega_r}{\delta_{sw}} = \frac{\omega_r}{\delta_f \times i} = \frac{u/L}{1 + \frac{m}{L^2} \times \left(\frac{a}{k_r} - \frac{b}{k_f} \right) u^2 \times i} \tag{14}$$

where, G_{sw} is steady yaw rate gain, ω_r is the yaw rate, u is vehicle speed, L is the wheelbase, m is vehicle mass, a is the distance from center of mass to front axle, b is the distance from center of mass to rear axle, k_f is lateral stiffness of front wheels, k_r is lateral stiffness of rear wheels, the other symbols are the same as above.

The transmission ratio for steering system can be recalculated by following equation.

$$i = \frac{\delta_{sw}}{\delta_f} = \frac{u/L}{1 + \frac{m}{L^2} \left(\frac{a}{k_r} - \frac{b}{k_f} \right) u^2} \cdot \frac{1}{G_{sw}} \tag{15}$$

where, the symbols are the same as above.

The ideal variable transmission ratio is affected by yaw rate gain significantly. The yaw rate gain of 0.24, 0.28, 0.32 and 0.36 are taken as examples, and the ideal variable transmission ratio curves for four different values can be obtained, as Fig. 11.

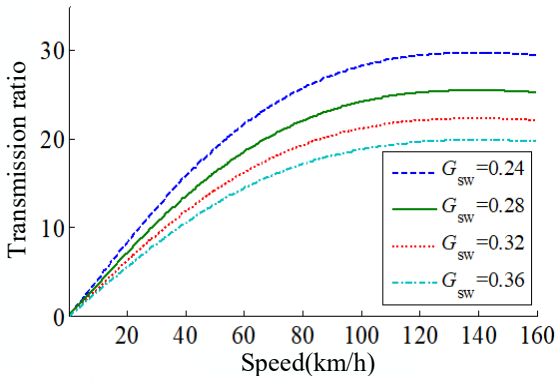

Fig. 11. Variable transmission ratio curves for different yaw rate gain

The results indicate that the ideal variable transmission ratio curve vary with the change of yaw rate gain, leading to varying degrees of sensitivity and stability in the steering system across different speeds [15]. The optimization algorithm is used to select yaw rate gain value based on comprehensive evaluation index of handling stability, and it can be calculated by following equation.

$$J_T = \sqrt{\frac{w_E J_E^2 + w_B J_B^2 + w_R J_R^2 + w_S J_S^2}{w_E + w_B + w_R + w_S}} \tag{16}$$

where, J_T is the comprehensive evaluation index of handling stability, J_E is the trajectory tracking error index, w_E is the weight of trajectory tracking error index, J_b is the variance for steering wheel speed, w_B is the weight of steering wheel speed variance, J_R is the rollover risk index, w_R is the weight of vehicle rollover risk index. J_S is the sideslip risk index, w_S is the weight of sideslip risk index.

As an optimization algorithm with strong robustness, genetic algorithm can adjust the search strategy adaptively, and has strong local and global search ability [16]. For that, it can satisfy the optimization of the yaw rate gain under different vehicle speeds. The comprehensive evaluation index is taken as the objective function and yaw rate gain is

taken as the optimization variable. Its operation flow is as Fig. 12, and the optimization results are shown in Table III.

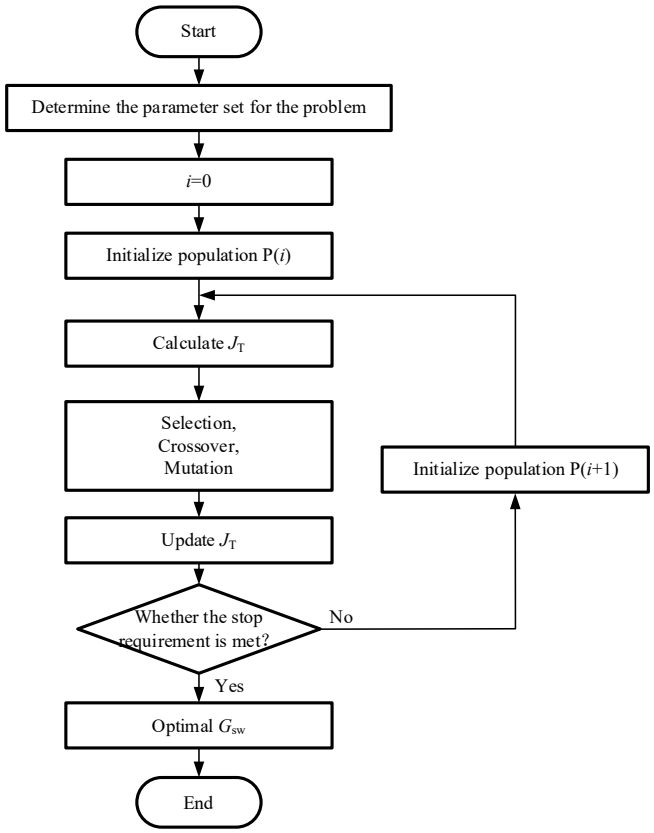

Fig. 12. Flow of genetic algorithm

TABLE III
OPTIMIZATION RESULTS OF YAW RATE GAIN AT DIFFERENT VEHICLE SPEEDS

Speed(km/h)	20	40	60	80	100	120
G_{sw}	0.83	0.69	0.52	0.36	0.30	0.19

When the optimization result of the yaw rate gain is 0.3, the corresponding variable transmission ratio curve is shown in Fig. 13.

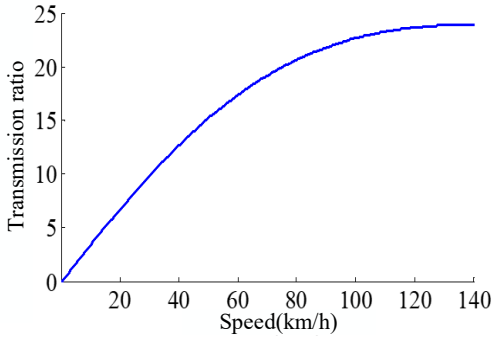

Fig. 13. Variable transmission ratio curve

If the steering system's transmission ratio is too low, the steering sensitivity of vehicle is large at low speed. For that, the lower limit value should be set for the variable transmission ratio curve. If the transmission ratio is too large, the steering sensitivity of vehicle is small at high speed. For that, the upper limit value should be set for the variable transmission ratio curve [17]. The ideal variable transmission ratio, based on the above requirements, is determined by the following equation.

$$i=\begin{cases}10.5 & (0\le u\le 30)\\ \dfrac{u/L}{1+\dfrac{m}{L^2}\left(\dfrac{a}{k_r}-\dfrac{b}{k_f}\right)u^2}\cdot\dfrac{1}{G_{sw}} & (30<u<90)\\ 23.5 & (90\le u)\end{cases} \tag{17}$$

where, the symbols are the same as above.

The segmentation curve for ideal variable transmission ratio can be obtained by equation 17, and it is shown as follows.

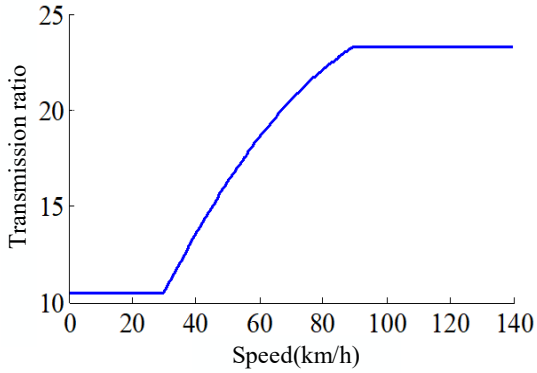

Fig. 14. The segmentation curve for ideal variable transmission ratio

B. Correction of the ideal variable transmission ratio curve

The ideal variable transmission ratio curve is modeled using the sine function fitting method [18]. The fitting equation is shown as follows, and the fitting curve is as Fig. 15.

$$i=(i_{max}-i_{min})/(1+e^{-\frac{u-(u_1+u_2)/2}{15}})+i_{min} \tag{18}$$

where, i_{max} is the upper limit of steering transmission ratio, i_{min} is the lower limit of steering transmission ratio, u_1 is lower critical speed, u_2 is upper critical speed, the other symbols are the same as above.

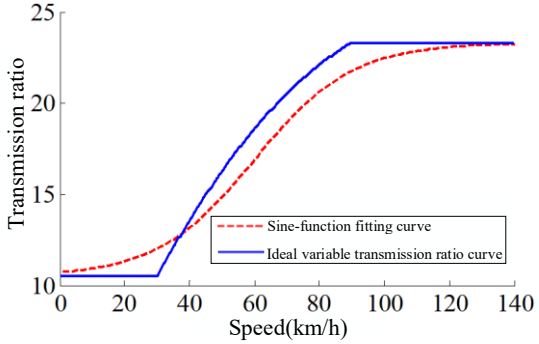

Fig. 15. Sine function fitting curve

As Fig. 15, the deviation between variable transmission ratio curve fitted by sine function and ideal variable transmission ratio curve is large. For that, fitting equation based on sine function needs to be corrected further, and the improved fitting equation is as follows.

$$i = \frac{\left(i_{\max} - i_{\min}\right)}{\left(1 + e^{-\varepsilon(u-\tau)}\right)} + i_{\min} \tag{19}$$

where, ε and τ are the variable transmission ratio curve adjustment coefficients, the other symbols are the same as above.

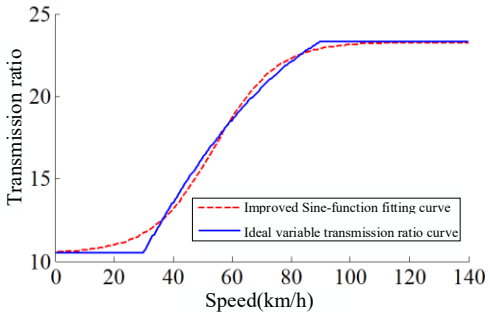

Fig. 16. Improved sine function fitting curve

The variable transmission ratio obtained by the improved fitting equation is shown in Fig. 16. The deviation after 30km/h is eliminated basically.

C. *Ideal variable transmission ratio design considering change of road adhesion coefficient*

The road adhesion coefficient is one of key factors affecting the handling stability of vehicle [19]. When traveling at the same speed, variations in road friction can cause substantial changes in yaw rate response and the optimal variable transmission ratio. If a constant ideal variable transmission ratio curve is used, it will result in a poor handling stability of vehicle on some road [20]. Therefore, a fuzzy controller is utilized to calculate yaw rate gain values and ideal variable transmission ratio curves that are suitable for various road adhesion coefficients.

1) *Membership function design:* The universe of road adhesion coefficient is set to {0, 1, 2, 3, 4, 5}. The universe of change rate of the road adhesion coefficient is set to {-2, -1, 0, 1, 2}. T is the sampling period. The universe of ideal yaw rate gain is set to {0.18, 0.22, 0.26, 0.31, 0.35}. Membership function of the input and output are shown in Fig. 17.

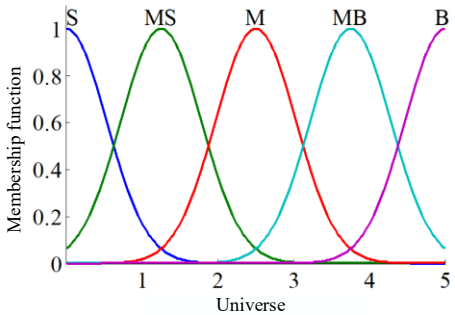

(a) Road adhesion coefficient

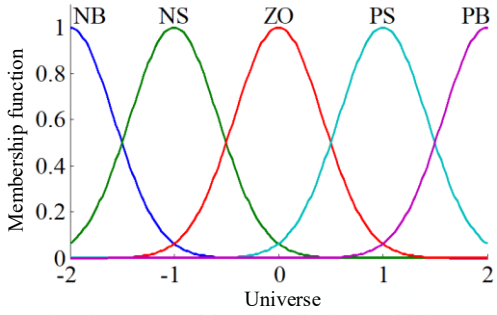

(b) Change rate of the road adhesion coefficient

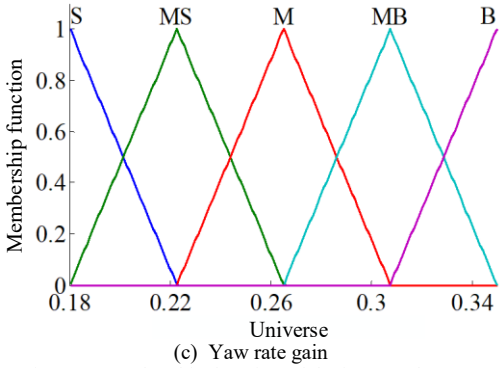

(c) Yaw rate gain

Fig. 17. Membership function of the input and output

2) *Fuzzy rules:* According to the relationship between road adhesion coefficients and vehicle handling stability, the yaw rate gain value should be smaller on the low adhesion coefficient road, and it should be lager on the high adhesion coefficient road. The corresponding fuzzy rules are designed, as Table IV.

TABLE IV
FUZZY RULES OF YAW RATE GAIN

Yaw rate gain		Change rate of the road adhesion coefficient				
		NB	NS	ZO	PS	PB
Road adhesion coefficient	S	S	S	S	MS	M
	MS	S	S	MS	M	M
	M	MS	M	M	M	MB
	MB	M	M	MB	MB	B
	B	M	MB	B	B	B

V. VERIFICATION AND ANALYSIS

A. *Verification platform*

For verifying the effectiveness of ideal variable transmission ratio considering the change of road adhesion coefficient, the verification simulation platform is built based on MATLAB/Simulink and CarSim. The schematic diagram is as Fig 18. The driver model, in-wheel motor model, yaw speed fuzzy controller, ideal variable transmission ratio calculation model and steering system model are built in MATLAB/Simulink. The body model, suspension model and tire model of the in-wheel motor electric vehicle are built in CarSim. MATLAB/Simulink receives the information of speed and road adhesion coefficient from CarSim, and sends the drive torque and front wheel steering angle to CarSim.

B. *Low adhesion coefficient road*

For verifying the impact of the ideal variable transmission ratio for handling stability when vehicle drives on the low adhesion coefficient road, the step input condition and continuous sine condition are utilized to verify the control effect.

1) *Step input condition:* The road adhesion coefficient is set as 0.2, the vehicle speed is set as 50 km/h. The steering wheel angle, front wheel angle, lateral acceleration and yaw rate as Fig. 19.

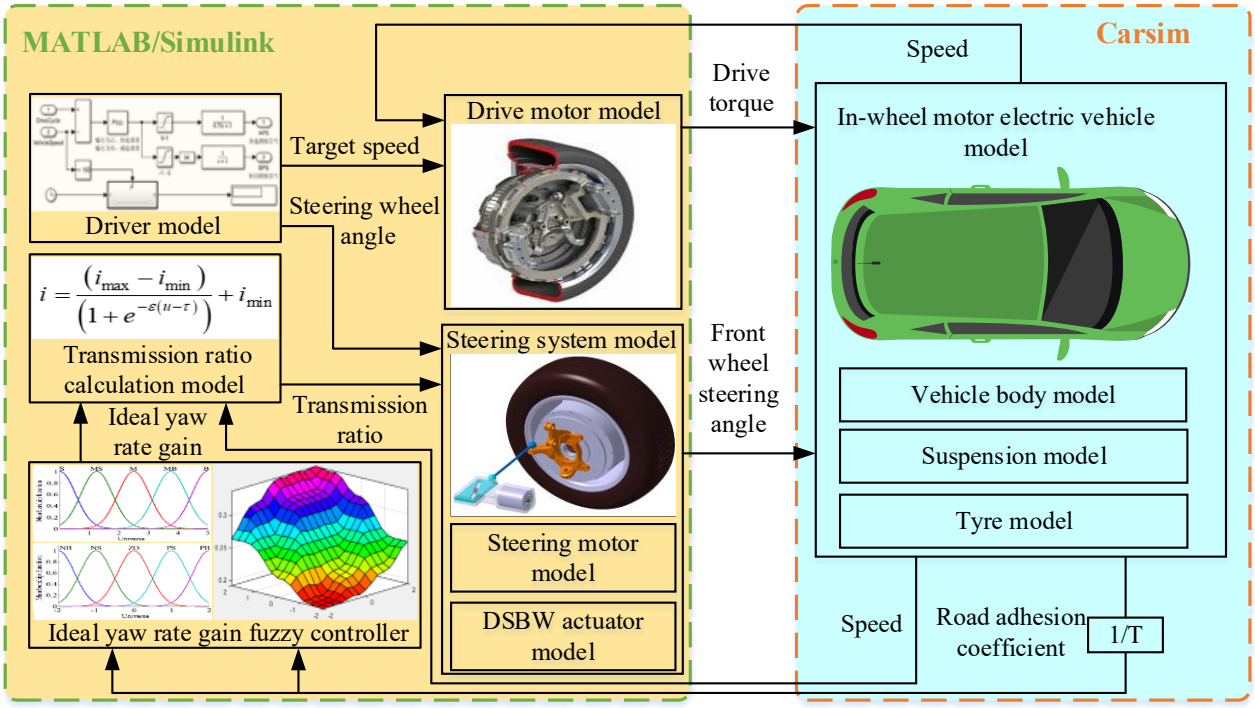

Fig. 18. Verification platform

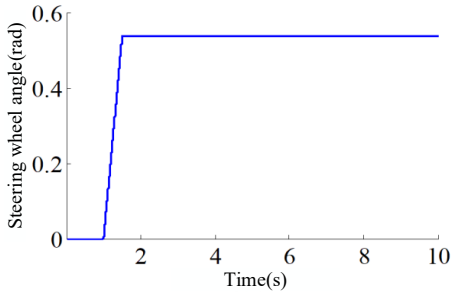

(a) Steering wheel angle

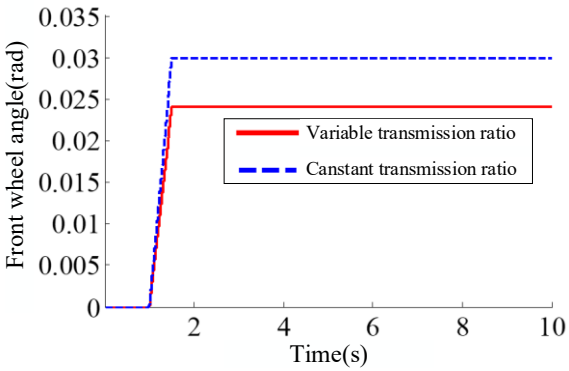

(b) Front wheel angle

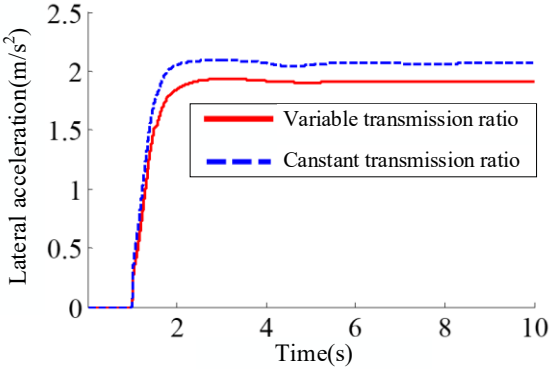

(c) Lateral acceleration

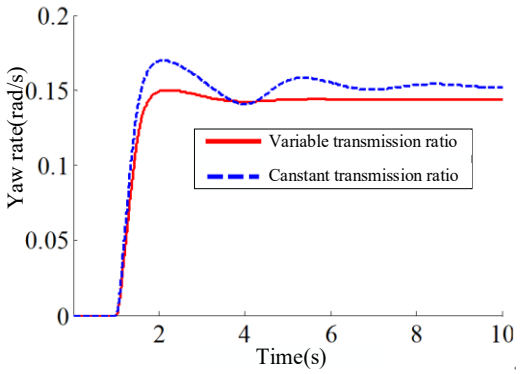

(d) Yaw rate

Fig. 19. Results of step input condition

As Fig 19 (b), the steady value for front wheel angle of constant transmission ratio is 0.030 rad, and the steady value for front wheel angle of variable transmission ratio is 0.024 rad. There is a 20% decrease in the constant value for the front wheel angle of the variable transmission ratio, and the steering sensitivity is reduced when driving on low adhesion coefficient roads. As Fig 19 (c), the steady value for lateral acceleration of constant transmission ratio is 2.07 m/s2, and the steady value for lateral acceleration of variable transmission ratio is 1.91 m/s2. The steady value for lateral acceleration of variable transmission ratio control is reduced by 7.7%. The peak value for lateral acceleration of constant transmission ratio is 2.13 m/s2, and the peak value for lateral acceleration of variable transmission ratio is 1.97 m/s2. The peak value for lateral acceleration of variable transmission ratio control is reduced by 7.5%. According to steady and peak value for lateral acceleration, the vehicle stability is improved significantly. As Fig 19 (d), the steady value for yaw rate of constant transmission ratio is 0.15 rad/s, and steady value for yaw rate of variable transmission ratio is 0.14 rad/s. The steady value for yaw rate value of variable transmission ratio is reduced by 7.1%. The peak value for yaw rate of constant transmission ratio is 0.17 rad/s, and the peak value for yaw rate of variable transmission ratio is 0.15

rad/s. The peak value for yaw rate of variable transmission ratio is reduced by 13.3%. The vehicle's stability has greatly improved based on the yaw rate's peak and stable values.

2) *Continuous sine condition:* The road adhesion coefficient is set as 0.2, the vehicle speed is set as 60 km/h. The steering wheel angle, front wheel angle, lateral acceleration and yaw rate are as Fig. 20.

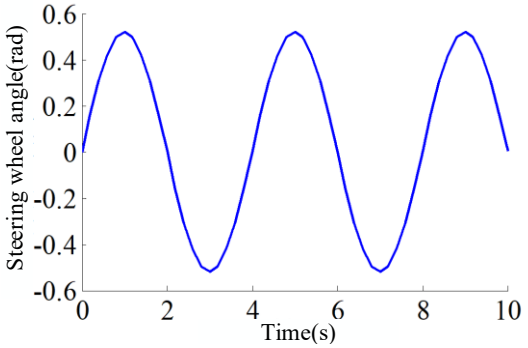

(a) Steering wheel angle

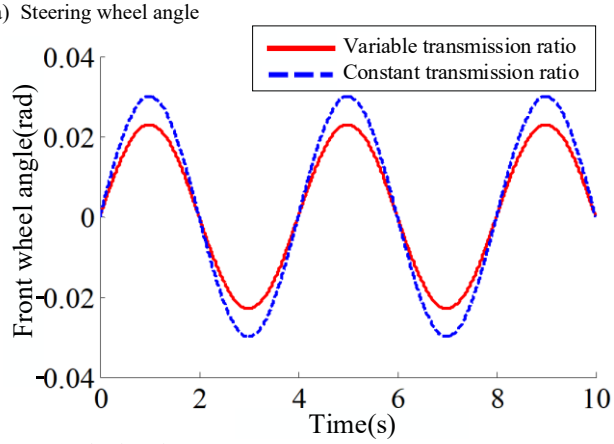

(b) Front wheel angle

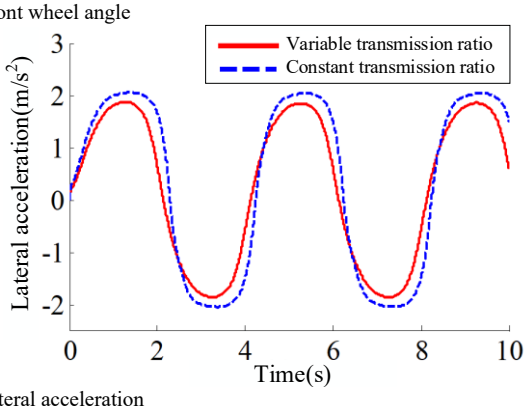

(c) Lateral acceleration

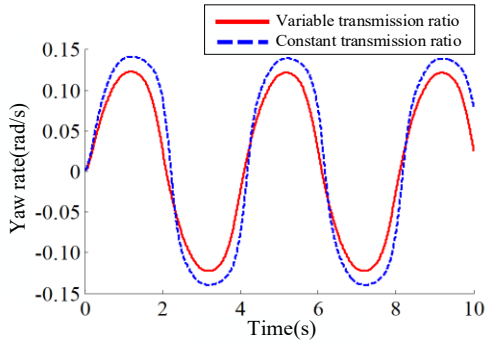

(d) Yaw rate

Fig. 20. Results of continuous sine condition

As Fig. 20 (b), the peak value for front wheel angle of constant transmission ratio is 0.030 rad, and the peak value for front wheel angle of variable transmission ratio is 0.022 rad. The peak value for front wheel of variable transmission ratio angle is reduced by 26.7%, the steering sensitivity is reduced, and the vehicle stability is improved significantly. As Fig. 20 (c), the peak value for lateral acceleration of constant transmission ratio is 2.05m/s2, and the peak value for lateral acceleration of variable transmission ratio is 1.87m/s2. The peak value for lateral acceleration of variable transmission ratio is reduced by 8.7%, and the vehicle stability is improved significantly. As Fig. 20 (d), the peak value for lateral acceleration of constant transmission ratio is 2.05rad/s, and the peak value for lateral acceleration of variable transmission ratio is 1.87rad/s. The vehicle's stability is greatly enhanced, and the variable transmission ratio's peak value for lateral acceleration is decreased by 8.7%.

3) *Fishhook maneuver test:* The road adhesion coefficient is set as 0.2, the vehicle speed is set as 50 km/h. The steering wheel angle, yaw rate, sideslip angle and lateral acceleration are shown in Fig. 21.

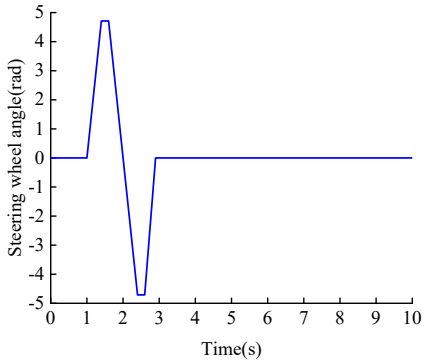

(a) Steering wheel angle

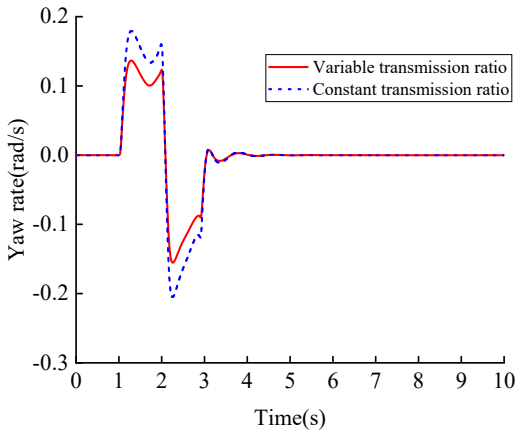

(b) Yaw rate

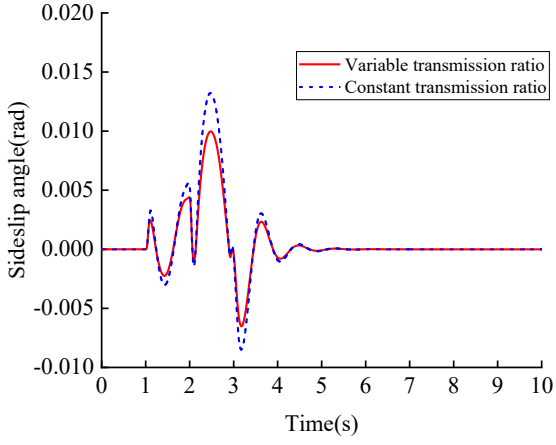

(c) Sideslip angle

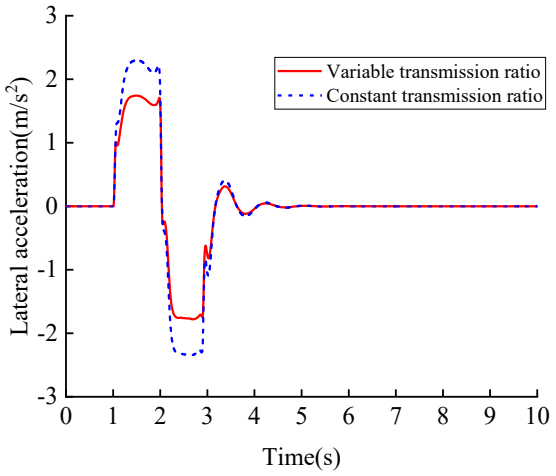

(d) Lateral acceleration

Fig. 21. Results of fishhook maneuver test

The steering wheel angle as Fig. 21 (a), at the onset of the experiment, the steering wheel angle is 0 rad, the steering wheel angle is turned to 5 rad at 1s, then the steering wheel angle is quickly changed to -5 rad, and the steering wheel gradually returned to the right position at 3 s. As shown in Fig. 21 (b), the peak value for yaw rate of constant transmission ratio is 0.19 rad/s, and the peak value for yaw rate of variable transmission ratio is 0.13 rad/s. The peak value for yaw rate of variable transmission ratio angle is reduced by 31.6%, the steering sensitivity is reduced, and the vehicle stability is improved significantly. As Fig. 21 (c), the peak value for sideslip angle of constant transmission ratio is 0.014 rad, and the peak value for sideslip angle of variable transmission ratio is 0.010 rad. The peak value for sideslip angle of variable transmission ratio is reduced by 28.6%, and the vehicle stability is improved significantly. As Fig. 21 (d), the peak value for lateral acceleration of constant transmission ratio is 2.31m/s^2, and the peak value for lateral acceleration of variable transmission ratio is 1.87 m/s^2. The peak value for lateral acceleration of variable transmission ratio is reduced by 19%, and the vehicle stability is enhanced significantly.

4) *Steady circular test:* The road adhesion coefficient is set as 0.2, the steering wheel angle is set as 0.785rad, and the vehicle speed accelerated from 20 km/h to 100 km/h in 100s gradually. The vehicle trajectory, yaw rate and sideslip angle as Fig. 22.

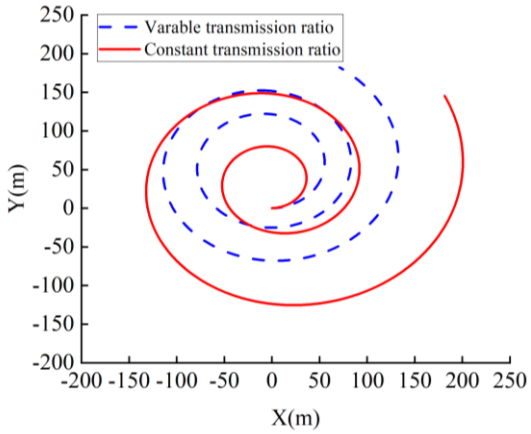

(a) Vehicle trajectory

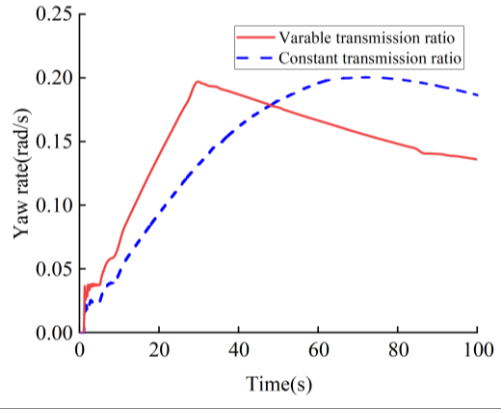

(b) Yaw rate

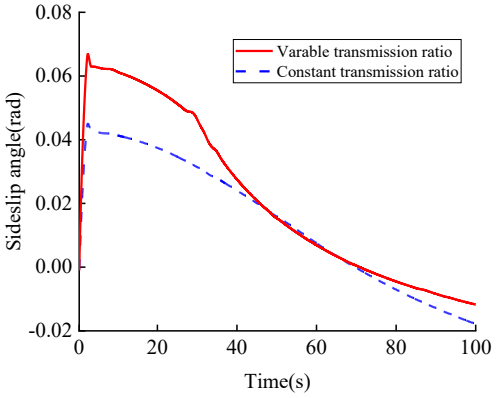

(c) Sideslip angle

Fig. 22. Result of steady circular test

As shown in Fig. 22 (a), the turning radius of the variable transmission ratio scheme is smaller than the turning radius of the constant transmission ratio scheme at low speeds. As the vehicle speed up, the turning radius of the variable transmission ratio scheme becomes larger than that of the constant transmission ratio scheme at high speed. As Fig. 22 (b), the peak yaw rate of the variable transmission ratio scheme is 0.20 rad/s, the peak yaw rate of the constant transmission ratio scheme is 0.17 rad/s, and the maneuverability and steering flexibility of the variable transmission ratio scheme are better than constant transmission ratio scheme when vehicle speed is 20-50 km/h. The yaw rate of the variable transmission ratio scheme is less than the yaw rate of the constant transmission ratio scheme, and the handling stability of the variable transmission ratio scheme is better than constant transmission ratio scheme when vehicle speed is 50-100 km/h. As shown in Fig. 22 (c), the peak sideslip angle of the variable transmission ratio scheme is 0.063 rad, the sideslip angle of the constant transmission ratio scheme is 0.043 rad, and the maneuverability and steering flexibility of the variable transmission ratio scheme are better than the constant transmission ratio scheme when vehicle speed is 20-50 km/h. The sideslip angle of the variable transmission ratio scheme is less than the sideslip angle of the constant transmission ratio scheme, and the handling stability of the variable transmission ratio scheme is better than the constant transmission ratio scheme when vehicle speed is 50-100km/h.

C. High adhesion coefficient road

1) *Step input condition:* The road adhesion coefficient is set to 0.85. The vehicle speeds are set as 30 km/h, 60 km/h, and 90 km/h respectively. The steering wheel angle, front

wheel angle, lateral acceleration and yaw rate at each speed are shown in Fig. 23, 24 and 25.

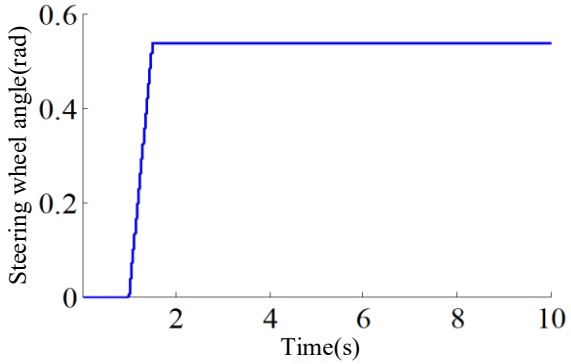

(a) Steering wheel angle

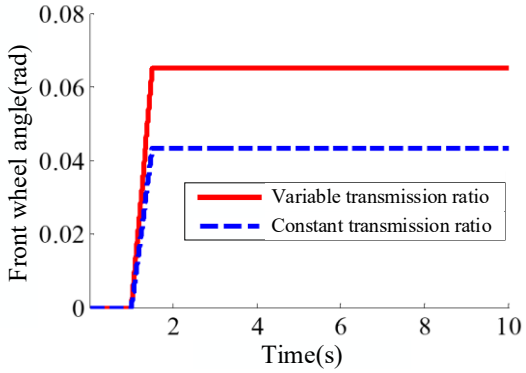

(b) Front wheel angle

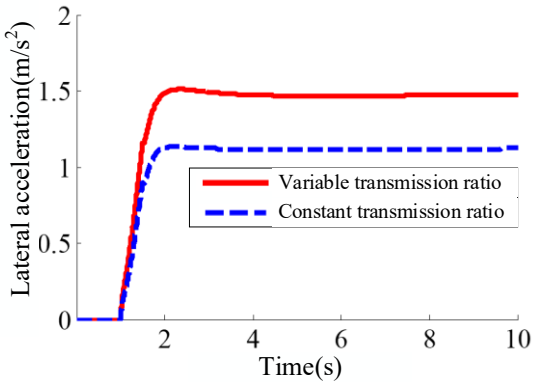

(c) Lateral acceleration

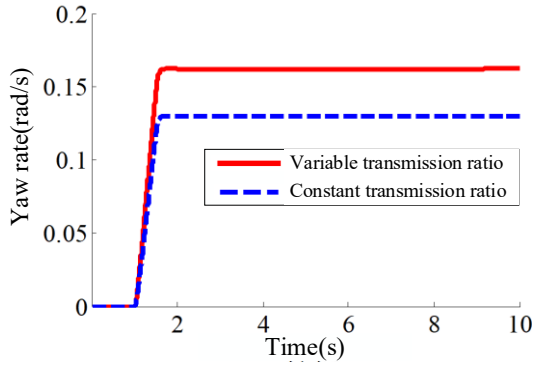

(d) Yaw rate

Fig. 23. Result of step input condition at 30km/h

As Fig. 23 (b), the steady value for front wheel angle of constant transmission ratio is 0.043rad, and the steady value for front wheel angle of variable transmission ratio is 0.065rad. The steady value for front wheel angle of variable transmission ratio is increased by 33.8%. The front wheel angle of ideal variable transmission ratio is larger at low speed, and the steering sensitivity is better than constant transmission ratio. As Fig. 23 (c), the steady value for lateral acceleration of constant transmission ratio is 1.12 m/s2, and the steady value for lateral acceleration of variable transmission ratio is 1.46 m/s2. The steady value for lateral acceleration of variable transmission ratio is increased by 23.2%. The peak value for lateral acceleration of constant transmission ratio is 1.18 m/s2, and the peak value for lateral acceleration of variable transmission ratio is 1.53m/s2. The peak value for lateral acceleration of variable transmission ratio control is increased by 29.6%. The lateral acceleration of ideal variable transmission ratio is larger at low speed, and the steering sensitivity is better than constant transmission ratio. As shown in Fig. 23 (d), the steady value for yaw rate of constant transmission ratio is 0.13 rad/s and the steady value for yaw rate of variable transmission ratio is 0.16 rad/s. The steady value for yaw rate of variable transmission ratio is increased by 18.7%. The peak value for yaw rate of constant transmission ratio is 0.13 rad/s, and the peak value for yaw rate of variable transmission ratio is 0.17 rad/s. The peak value for yaw rate of variable transmission ratio is increased by 23.5%. The yaw rate of ideal variable transmission ratio is larger at low speed, and the steering sensitivity is better than constant transmission ratio.

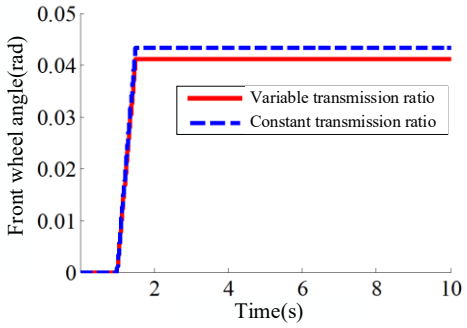

(a) Front wheel angle

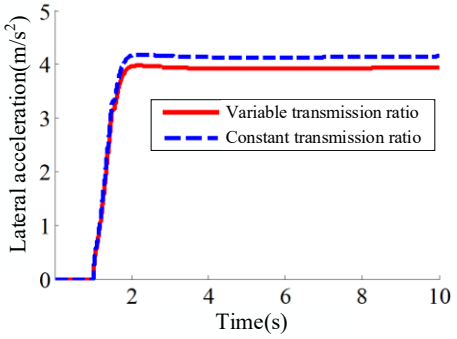

(b) Lateral acceleration

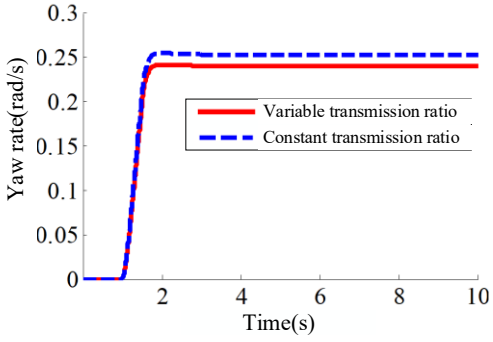

(c) Yaw rate

Fig. 24. Result of step input condition at 60km/h

As Fig. 24 (a), the steady front wheel angle of constant transmission ratio is 0.044rad, the steady value for front wheel angle of variable transmission ratio is 0.041rad, and the difference is within 4.6%. At most time, their front wheel angle is the same. As Fig. 24 (b), the steady value for lateral acceleration of constant transmission ratio is 4.12 m/s^2, the steady value for lateral acceleration of variable transmission ratio is 3.92 m/s^2, and the difference is within 4.8%. At most time, their lateral acceleration is the same. As shown in Fig. 24 (c), the steady value for yaw rate of constant transmission ratio is 0.25 rad/s, the steady value for yaw rate of variable transmission ratio 0.24 rad/s, and the difference is within 4.0%. At most time, their yaw rate is the same.

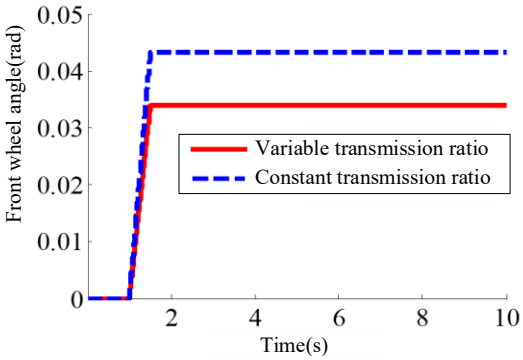

(a) Front wheel angle

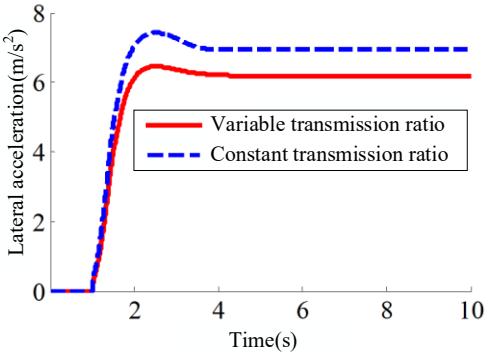

(b) Lateral acceleration

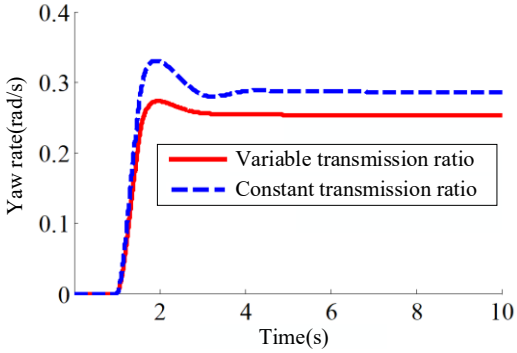

(c) Yaw rate

Fig. 25. Response curve at 90km/h

As Fig. 25 (a), the steady value for front wheel angle of constant transmission ratio is 0.043 rad, and steady value for front wheel angle of variable transmission ratio is 0.033 rad. The steady value for the front wheel angle of the variable transmission ratio drops by 23.3%. At high speed, the front wheel angle for the ideal variable transmission ratio is smaller. This leads to better handling stability compared to a constant transmission ratio. As Fig. 25 (b), the steady value for lateral acceleration of constant transmission ratio is 6.91 m/s2, and the steady value for lateral acceleration of variable transmission ratio is 6.16 m/s2. The steady value for lateral acceleration of variable transmission ratio is reduced by 10.9%. The peak value for lateral acceleration of constant transmission ratio is 7.55 m/s2, and the peak value for lateral acceleration of variable transmission ratio is 6.24 m/s2. The peak value for lateral acceleration of variable transmission ratio control is reduced by 17.4%. The lateral acceleration of ideal variable transmission ratio is smaller at high speed, and the handling stability is better than constant transmission ratio. As Fig. 25 (c), the steady value for yaw rate of constant transmission ratio is 0.29rad/s and the steady value for yaw rate of variable transmission ratio is 0.25rad/s. The steady value for yaw rate of variable transmission ratio is reduced by 12.2%. The peak value yaw rate of constant transmission ratio is 0.33 rad/s, and the peak value for yaw rate of variable transmission ratio is 0.27 rad/s. The peak value for yaw rate of variable transmission ratio is reduced by 18.2%. The yaw rate of ideal variable transmission ratio is smaller at high speed, and the handling stability is better than constant transmission ratio.

2) *Continuous sine condition:* The road adhesion coefficient is set as 0.85. The vehicle speed is set as 30 km/h, 60 km/h, and 90 km/h respectively. The steering wheel angle, the front wheel angle, lateral acceleration and yaw rate response at each speed are shown in Fig. 26 ,27 and 28.

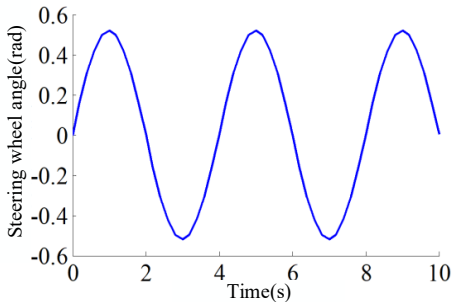

(a) Steering wheel angle

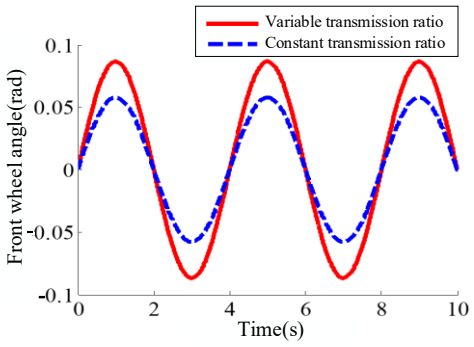

(b) Front wheel angle

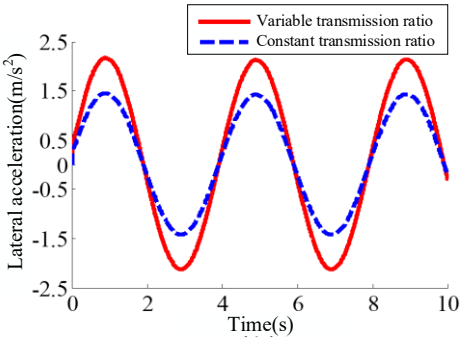

(c) Lateral acceleration

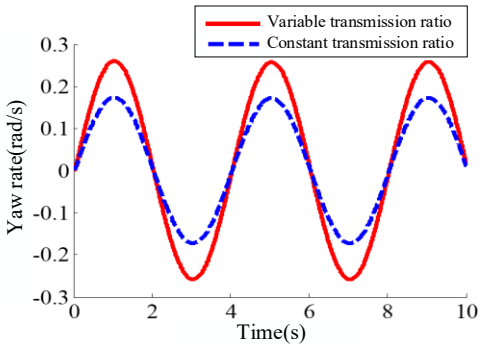

(d) Yaw rate

Fig. 26. Result of continuous sine condition at 30km/h

As Fig 26 (b), the peak value for front wheel angle of constant transmission ratio is 0.05 rad, and the peak value for front wheel angle of variable transmission ratio is 0.08 rad. The peak value for front wheel angle of variable transmission ratio is increased by 37.5%. The front wheel angle of ideal variable transmission ratio is larger at low speed, and the steering sensitivity is better than constant transmission ratio. As Fig 26 (c), the peak value for lateral acceleration of constant transmission ratio is 1.41 m/s^2, and the peak value for lateral acceleration of variable transmission ratio is 2.11 m/s^2. The peak value for front wheel angle of variable transmission ratio is increased by 33.1%. The lateral acceleration of ideal variable transmission ratio is larger at low speed, and the steering sensitivity is better than constant transmission ratio. As shown in Fig. 26 (d), the peak value for yaw rate of constant transmission ratio is 0.17 rad/s, and the peak value for yaw rate of variable transmission ratio is 0.26 rad/s. The peak value for yaw rate of variable transmission ratio is increased by 34.6%. The yaw rate of ideal variable transmission ratio is larger at low speed, and the steering sensitivity is better than constant transmission ratio.

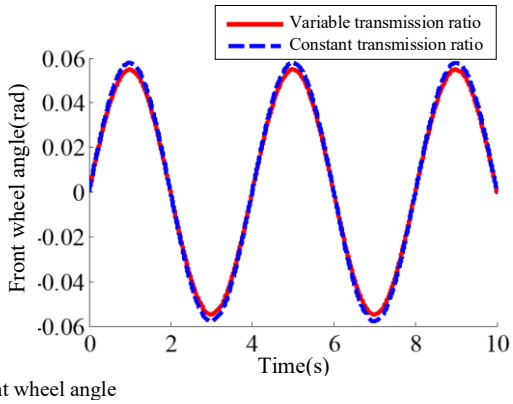

(a) Front wheel angle

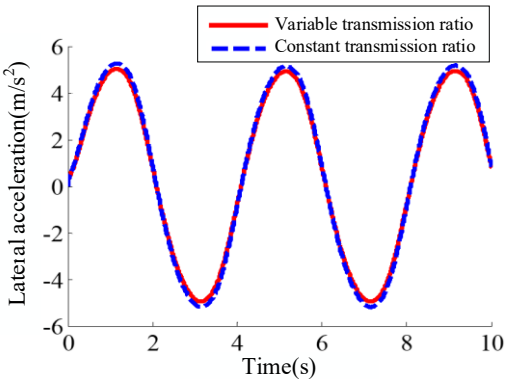

(b) Lateral acceleration

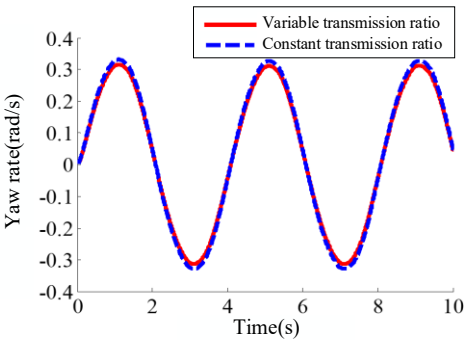

(c) Yaw rate

Fig. 27. Result of continuous sine condition at 60km/h

As Fig 27 (a), the peak value for front wheel angle of constant transmission ratio is 0.044 rad, the peak value for front wheel angle of variable transmission ratio is 0.041 rad, and their difference is less than 4.6%. At most time, their front wheel angle is the same. As Fig 27 (b), the peak value for lateral acceleration of constant transmission ratio is 4.12 m/s^2, the peak value for lateral acceleration of variable transmission ratio is 3.92 m/s^2, and their difference is less than 4.8%. At most time, their lateral acceleration is the same. As shown in Fig 27 (c), the peak value for yaw rate of constant transmission ratio is 0.25 rad/s, the peak value for yaw rate of variable transmission ratio is 0.24 rad/s, and their difference is less than 4.0%.

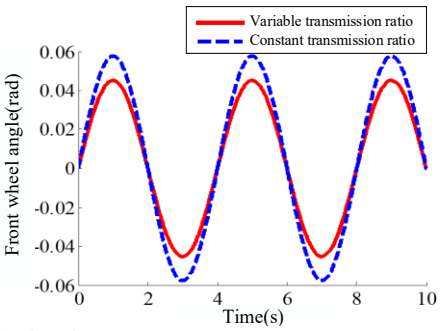

(a) Front wheel angle

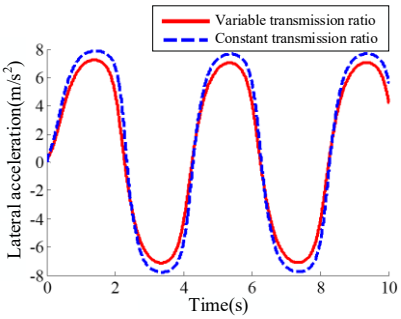

(b) Lateral acceleration

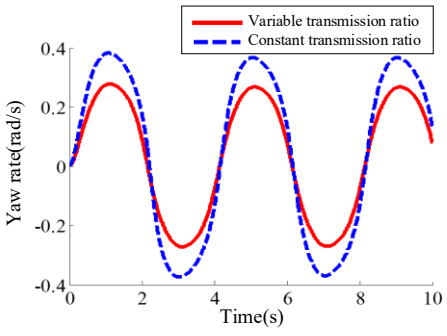

(c) Yaw rate

Fig. 28. Result of continuous sine condition at 90km/h

As Fig. 28 (a), the peak value for front wheel angle of constant transmission ratio is 0.057 rad, and the peak value for front wheel angle of variable transmission ratio is 0.045 rad. The peak value for front wheel angle of variable transmission ratio is reduced by 21%. The front wheel angle of ideal variable transmission ratio is smaller at high speed, and the handling stability is better than constant transmission ratio. As Fig. 28 (b), the peak value for lateral acceleration of constant transmission ratio is 7.41 m/s2, and the peak value for lateral acceleration of variable transmission ratio is 6.44 m/s2. The peak value for lateral acceleration of variable transmission ratio is reduced by 13.1%. The lateral acceleration of ideal variable transmission ratio is smaller at high speed, and the handling stability is better than constant transmission ratio. As Fig. 28 (c), the peak value for yaw rate of constant transmission ratio is 0.38 rad/s, and the peak value for yaw rate of variable transmission ratio is 0.26 rad/s. The peak value for yaw rate of variable transmission ratio is reduced by 31.5%. The yaw rate of ideal variable transmission ratio is smaller at high speed, and the handling stability is better than constant transmission ratio.

3) *Fishhook maneuver test:* The road adhesion coefficient is set as 0.85. The vehicle speed is set as 30 km/h and 60 km/h respectively. The steering wheel angle, yaw rate, sideslip angle and lateral acceleration and are shown in Fig. 29 and 30.

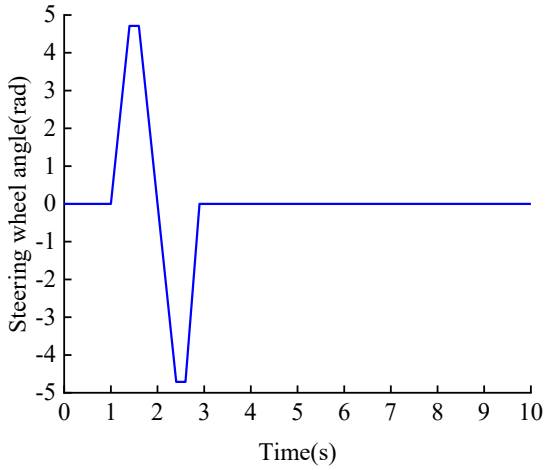

(a) Steering wheel angle

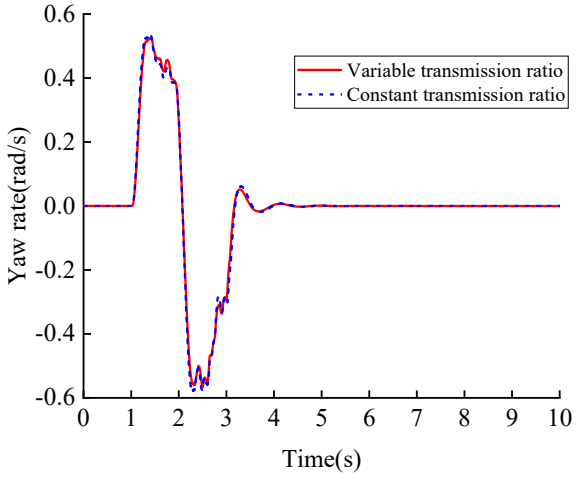

(b) Yaw rate

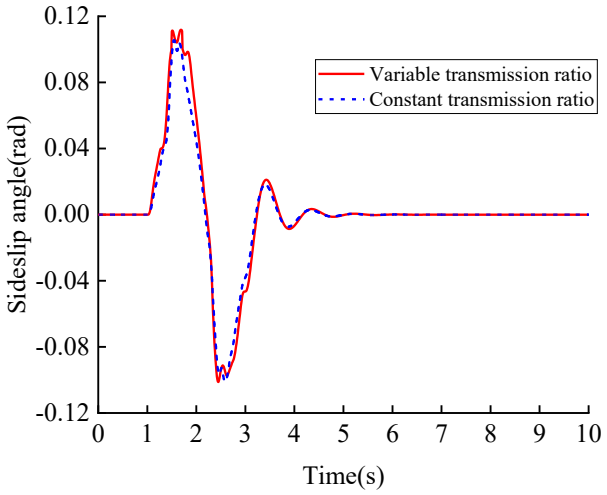

(c) Sideslip angle

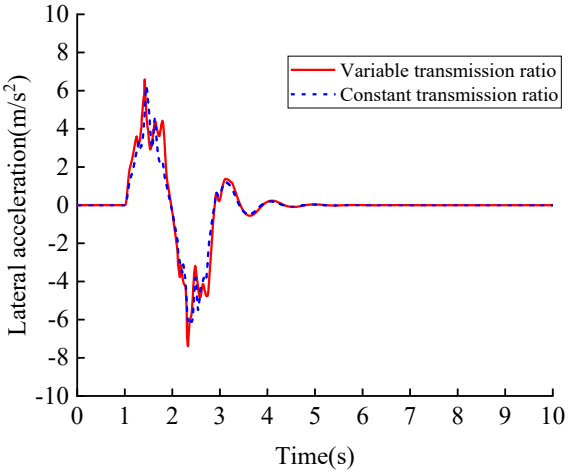

(d) Lateral acceleration

Fig. 29. Results of fishhook maneuver test at 30km/h

The steering wheel angle as Fig. 29 (a), at the beginning of the test, the steering wheel angle is 0 rad, the steering wheel angle is turned to 5 rad at 1 s, then the steering wheel angle is quickly changed to -5 rad, and the steering wheel gradually return to the right position at 3 s. As Fig 29 (b), the peak value for yaw rate of constant transmission ratio is 0.526 rad/s, and the peak value for yaw rate of variable transmission ratio is 0.545 rad/s. The peak value for yaw rate of variable transmission ratio is increased by 3.6%. The yaw rate of variable transmission ratio is larger at low speed, and the steering sensitivity is better than the constant transmission ratio. As Fig. 29 (c), the peak value for sideslip angle of constant transmission ratio is 0.107 rad, and the peak value for sideslip angle of variable transmission ratio is 0.112 rad. The peak value for sideslip angle of variable transmission ratio is increased by 4.7%. The sideslip angle of ideal variable transmission ratio is larger at low speed, and the steering sensitivity is better than the constant transmission ratio. As Fig. 29 (d), the peak value for lateral acceleration of constant transmission ratio is 6.221 m/s^2, and the peak value for lateral acceleration of variable transmission ratio is 6.596 m/s^2. The peak value for lateral acceleration of variable transmission ratio is increased by 6.03%. The lateral acceleration of an ideal variable transmission ratio is higher at low speed. Also, it offers better steering sensitivity compared to a constant transmission ratio.

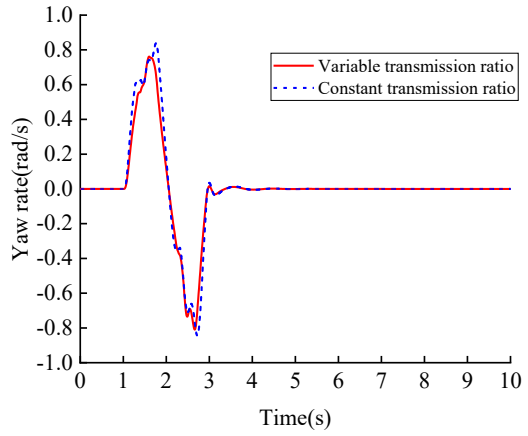

(a) Yaw rate

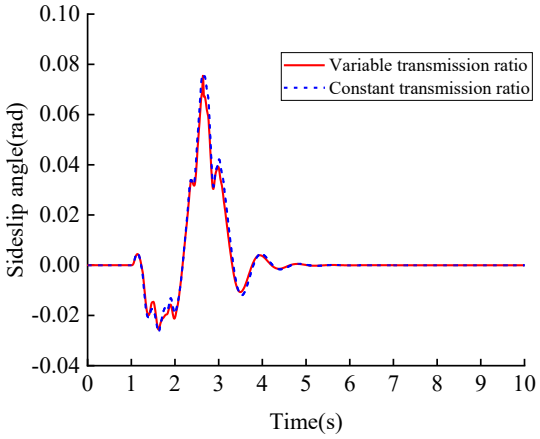

(b) Sideslip angle

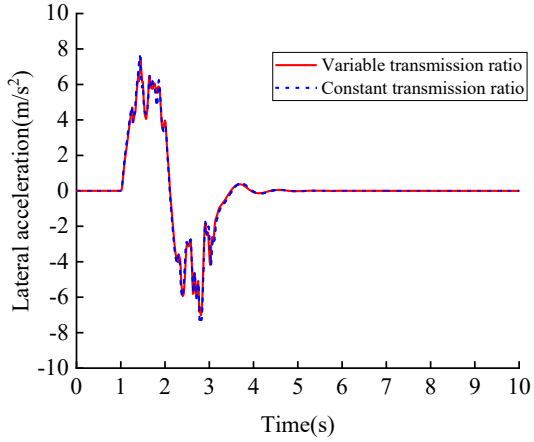

(c) Lateral acceleration

Fig. 30. Results of fishhook maneuver test at 60km/h

The steering wheel angle is same as Fig. 29 (a). As Fig 30 (a), the peak value for yaw rate of constant transmission ratio is 0.822 rad/s, the peak value for yaw rate of variable transmission ratio is 0.798 rad/s, and their difference is less than 3%. At most time, their yaw rate is the same. As Fig 30 (b), the peak value for sideslip angle of constant transmission ratio is 0.075 rad, the peak value for sideslip angle of variable transmission ratio is 0.074 rad, and their difference is less than 1.3%. At most time, their sideslip angle is the same. As shown in Fig 30 (c), the peak value for lateral acceleration of constant transmission ratio is 7.645 m/s^2, the peak value for lateral acceleration of variable transmission ratio is 7.486 m/s^2, and their difference is less than 2.08%. At most time, their lateral acceleration is the same.

4) *Steady circular test:* The road adhesion coefficient is set as 0.2, the steering wheel angle is set as 0.785rad. The vehicle speed accelerated from 20km/h to 100km/h in 100s gradually. Vehicle trajectory, yaw rate and sideslip angle are as Fig. 31.

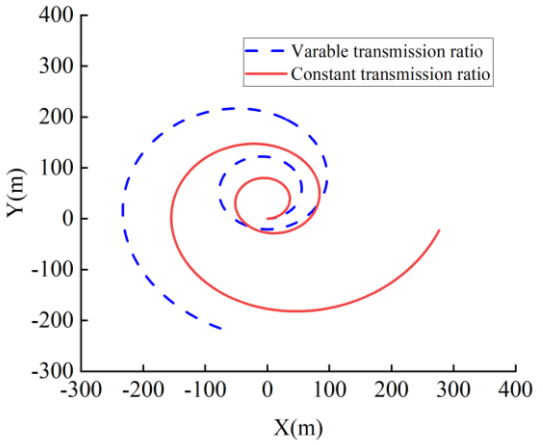

(a) Vehicle trajectory

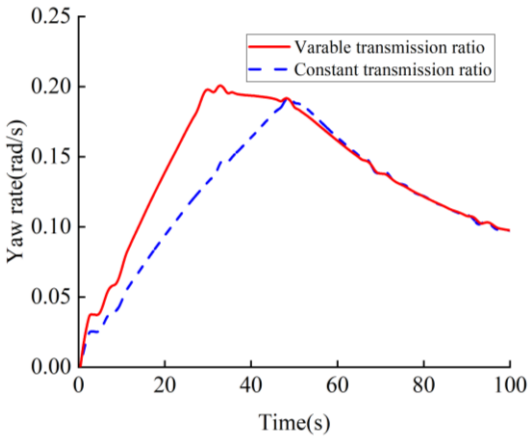

(b) Yaw rate

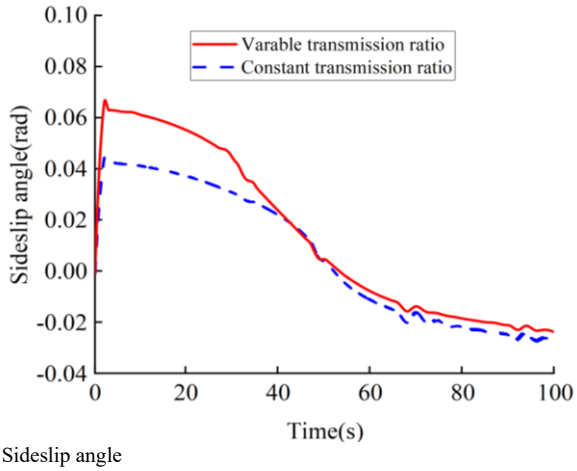

(c) Sideslip angle

Fig. 31. Result of steady circular test

As Fig. 31 (a), the turning radius of the variable transmission ratio scheme is smaller than the turning radius of the constant transmission ratio scheme at low speeds. As the vehicle speed up, the turning radius of the variable transmission ratio scheme becomes larger than that of the constant transmission ratio scheme at high speed. As Fig. 23 (b), the peak yaw rate of the variable transmission ratio scheme is 0.20 rad/s, the peak yaw rate of the constant transmission ratio scheme is 0.19 rad/s, and the maneuverability and steering flexibility of the variable transmission ratio scheme are better than constant transmission ratio scheme when vehicle speed is 20-50 km/h.

The yaw rate of the variable transmission ratio scheme is less than the yaw rate of the constant transmission ratio scheme, and the handling stability of the variable transmission ratio scheme is better than constant transmission ratio scheme when vehicle speed is 50-100 km/h. As Fig. 23 (c), the peak sideslip angle of the variable transmission ratio scheme is 0.064 rad, the sideslip angle of the constant transmission ratio scheme is 0.042 rad, and the maneuverability and steering flexibility of the variable transmission ratio scheme are better than constant transmission ratio scheme when vehicle speed is 20-50 km/h. The sideslip angle of the variable transmission ratio scheme is less than the sideslip angle of the constant transmission ratio scheme, and the handling stability of the variable transmission ratio scheme is better than constant transmission ratio scheme when vehicle speed is 50-100km/h.

In summary, under low-adhesion coefficient road conditions, the variable transmission ratio exhibits a smaller steady-state front wheel angle and superior steering sensitivity, with its yaw rate and lateral acceleration lower than those of fixed transmission ratio systems, thereby enhancing vehicle handling stability. On high-adhesion coefficient roads, at low speeds, the ideal variable transmission ratio features a greater front wheel angle and better steering sensitivity; during medium speeds, discrepancies in front wheel angle, yaw rate, and lateral acceleration are less significant; at high speeds, its front wheel angle and steering sensitivity decrease, accompanied by reduced yaw rate and lateral acceleration, further improving stability. Overall, the ideal variable transmission ratio effectively satisfies the requirements for steering sensitivity at low speeds and stability at high speeds.

VI. Conclusion

To enhance vehicle steering performance and leverage SBW benefits, a DSBW integrated fault-tolerant mechanism is proposed.

(1) A dual-motor DSBW scheme for in-wheel electric vehicle is proposed. It mainly consists of two steering motors, wedge block, ball screw, push rod and roller, etc. Aiming at the failure problem of DSBW, the fault-tolerant mechanism is designed, and the parameter matching and selection of main components are carried out based on the demand of DSBW. 3D model is built, and motion check is carried out based on CATIA and Adams/View. Based on the working principle, structural characteristics and power transmission route of DSBW, the motion constraints of each component and the load distribution of the assembly are analyzed. Taking the steering knuckle as example, the topological optimization is carried out for improving the steering response speed and reducing the material cost. The strength of the steering knuckle is checked based on uneven road condition, emergency braking condition and sideslip condition.

(2) For taking advantage of variable steering transmission ratio of DSBW, the comprehensive evaluation index considering vehicle rollover risk, vehicle handling stability, trajectory tracking error, and vehicle sideslip risk is studied on the basis of vehicle steering performance and handling stability. The ideal variable transmission ratio of DSBW considering yaw rate gain is studied. The optimal yaw rate gain is selected based on genetic algorithm, and the modified sine function is used to fit the ideal variable transmission ratio curve. For improving the adaptability of the steering transmission ratio to the road adhesion coefficient, the ideal variable transmission ratio on different adhesion coefficient roads is modified based on fuzzy control. The verification simulation platform is built based on MATLAB/Simulink and CarSim, and the control effect of the ideal variable transmission ratio is verified by continuous sine condition, step input condition, fishhook maneuver test and steady circular test. The results show that the ideal variable transmission ratio can meet the requirements of steering sensitivity at low speed and stability at high speed.

References

[1] H. H. Yang, W. T. Liu, L. Chen and F. Yu, “An adaptive hierarchical control approach of vehicle handling stability improvement based on Steer-by-Wire Systems.” *Mechatronics*, vol. 77, 2021.

[2] M. Irmer, R. Degen, A. Nüßgen, K. Thomas, H. Henrichfreise, and M. Ruschitzka, “Development and Analysis of a Detail Model for Steer-by-Wire Systems,” *IEEE Access*, vol. 11, pp. 7229-7236, 2023.

[3] B. DeBoer, J. B. Kimball and K. Bubbar, “Design, Control, and Validation of a Brake-by-Wire Actuator for Scaled Electric Vehicles.” *IEEE Robotics and Automation Letters*, vol. 9, no. 5, pp. 4695-4701, 2024.

[4] L. B. Chen and L. Tang, “Yaw stability control for steer-by-wire vehicle based on radial basis network and terminal sliding mode theory.” *Proceedings of the Institution of Mechanical Engineers, Part D: Journal of Automobile Engineering*, vol. 237, no. 8, pp. 2036-2048, 2023.

[5] G. B. Shi, P. F. Qiao, D. G. Sang, S. Wang and M. H. Song, “Synchronous and fault-tolerance control for dual-motor steer-by-wire system of commercial vehicle.” *Proceedings of the Institution of Mechanical Engineers, Part D: Journal of Automobile Engineering*, vol. 238, no. 7, pp. 1964-1980, 2024.

[6] A. Wang, C. Y. Wang, H. Zhang and W. Z. Zhao, “Steering energy optimisation strategy of steer-by-wire system with dual-motor.” *International Journal of Vehicle Design*, vol. 85, no. 2-4, pp. 115-138, 2021.

[7] W. L. Xu, Z. C. He, M. Mao, E. Li and Y. J. Chen, “Steering linkage topology design using angle-based block partitioning symmetric model (APSM).” *Structural and Multidisciplinary Optimization*, vol. 67, no. 10, p. 175, 2024.

[8] B. S. Shen, “Lightweight design of a steering power cylinder bracket.” *Advances in Mechanical Engineering*, vol. 16, no. 5, 2024.

[9] J. X. Lin, F. Zhang, L. Su, G. J. Song, Z. W. Liu and Y. Zhang, “Research on variable transmission ratio control method to improve vehicle handling comfort based on steer-by-wire system.” *Actuators*, vol. 13, no. 2, 2024.

[10] X. D. Wu and W. Q. Li, “Variable steering ratio control of steer-by-wire vehicle to improve handling performance.” *Proceedings of the Institution of Mechanical Engineers, Part D: Journal of Automobile Engineering*, vol. 234, no. 2-3, pp. 774-782, 2020.

[11] D. Cao, B. Tang, H. B. Jiang, C. H. Yin, D. Zhang and Y. Q. Huang, “Study on low-speed steering resistance torque of vehicles considering friction between tire and pavement.” *Applied Sciences*, vol. 9, no. 5, p. 1015, 2019.

[12] Z. Y. Wang, S. Wei, K. Bao, Y. Liu, S. Y. Peng and Q. Zhang, “Analysis of multiple failure behaviors of steering knuckle ball hinge of multi-axle heavy vehicle.” *Advances in Mechanical Engineering*, vol. 13, no. 10, 2021.

[13] S. Na, Z. P. Li, F. Qiu and C. Zhang, “Torque control of electric power steering systems based on improved active disturbance rejection control.” *Mathematical Problems in Engineering*, vol. 2020, 2020.

[14] Q. T. Li, J. Zhang, L. Li, X. Y. Wang, B. J. Zhang and X. Y. Ping, “Coordination control of maneuverability and stability for four-wheel-independent-drive EV considering tire sideslip.” *IEEE Transactions on Transportation Electrification*, vol. 8, no. 3, pp. 3111-3126, 2022.

[15] S. C. Zou, Z. K. Luan, W. Z. Zhao and C. Y. Wang, “Personalized design strategy of vehicle steer-by-wire characteristics considering driving style.” *Proceedings of the Institution of Mechanical Engineers, Part C: Journal of Mechanical Engineering Science*, vol. 237, no. 2, pp. 253-266, 2023.

[16] T. A. Anh Nguyen and J. Iqbal, "Genetic algorithm inspired optimal integrated nonlinear control technique for an electric power steering system." *Journal of the Brazilian Society of Mechanical Sciences and Engineering*, vol. 46, no. 11, pp.1-23, 2024.

[17] X. J. He, K. Yang, Y. L. Chang, C. Ma, W. Wang and J. Wang, "Analysis and control for ideal variable transmission ratio characteristics of active front wheel steering." *International Journal of Modelling, Identification and Control*, vol. 45, no. 1, pp.40-57, 2024.

[18] Q. Shi, Y. J. Wei, D. Xie, F. L. Li, K. Song and L. He, "A model predictive control approach for angle tracking of steer-by-wire system with nonlinear transmission ratio." *Asian Journal of Control*, vol. 25, no. 2, pp. 1156-1166, 2023.

[19] N. Y. Guo, X. D. Zhang, Y. Zou, B. Lenzo, G. D. Du and T. Zhang, "A supervisory control strategy of distributed drive electric vehicles for coordinating handling, lateral stability, and energy efficiency." *IEEE Transactions on Transportation Electrification*, vol. 7, no. 4, pp. 2488-2504, 2021.

[20] X. T. Liang, L. F. Zhao, Q. D. Wang, W. W. Chen, G. Xia, J. F. Hu and P. F. Jiang, "A novel steering-by-wire system with road sense adaptive friction compensation." *Mechanical Systems and Signal Processing*, vol. 169, 2022.